JOURNAL OF APPLIED ELECTROCHEMISTRY 13 (1983) 121–131

Melting-crystallization properties of the sulphur electrolyte in sodium-sulphur batteries

G. J. JANZ, D. J. ROGERS

Cogswell Laboratory, Rensselaer Polytechnic Institute, Troy, New York 12181, USA

Received 1 June 1982

The present communication reports the results of some melting-crystallization studies, undertaken to characterize the thermal behaviour of the sulphur electrolyte. Heat capacities, enthalpies of transition (solid-state) and of fusion have been measured. The electrolyte is observed to have glass forming tendencies and the composition range for this behaviour is characterized. An inverse-crystallization phenomenon is observed as the sulphur content increases. The saturation solubility of sulphur is the sodium pentasulphide layer in the liquid–liquid immiscibility composition range of the sulphur electrolyte, the influence of moisture as an additive in trace amounts, and the thermal character of the chemical events in the formation of polysulphides from sulphur and Na_2S as reactants are also reported.

1. Introduction

Basic to the concept of sodium–sulphur battery is the use of the sodium–sulphur couple in which a ceramic membrane (sodium ion conducting) separates the molten reactants of each electrode. The sodium–sulphur couple is attractive because of its relatively high theoretical energy density (346 Wh lb^{-1}), high open circuit voltage (2.08 V), and the abundance and intrinsic low cost of the reactants. Both reactants are molten at the operating temperature (~ 300–350° C). Since molten sulphur is not a conductor it is intimately mixed with some form of graphite/carbon, and this contacts the ceramic (tube) to permit initial operation. The sodium polysulphide, thus formed, is an ionic conductor, and this serves as a further secondary electrolyte, permitting high current density operations.

The composition range (~ 66 wt% to 100 wt% sulphur) and the temperature limits (~ 300–350° C) are illustrated in Fig. 1 as a shaded area superimposed on the phase diagram for this system [1–3]. In the charging process higher polysulphides and sulphur are formed, which equilibrate with the bulk sulphide phase by chemical reaction and diffusion. As the charging process continues, the composition range of liquid–liquid immiscibility is entered, in which a molten pentasulphide phase and a molten sulphur phase co-exist, each mutually saturated with the other component. In the discharging process, lower polysulphides are formed; these equilibrate with the bulk of the melt, taking up more sulphur, until the liquidus line for Na_2S_2 is reached (Fig. 1), and the Na_2S_2 no longer dissolves in the sulphur electrolyte, i.e., 'precipitation'. In the present work we report the results of some studies undertaken for the composition range from complete charge (100% wt sulphur) to total discharge (~ 66 wt% sulphur; i.e, Na_2S_2 liquidus). Heat capacities, heats of fusion, and of solid-state transition and the events during thermal cycling were investigated and the results are reported. The measurements were extended well into the two immiscible liquids composition range. The chemical events in the formation of polysulphides, as well as the influence of additives to the sulphur-electrolyte were also examined, and these aspects are also reported.

2. Measurements

2.1. *Melting–crystallization studies and thermal measurements*

The technique of DSC (differential scanning calorimetry) was selected as the basic experimental method; in the DSC technique it is poss-

0021–891X/83/010121–11$03.82/0

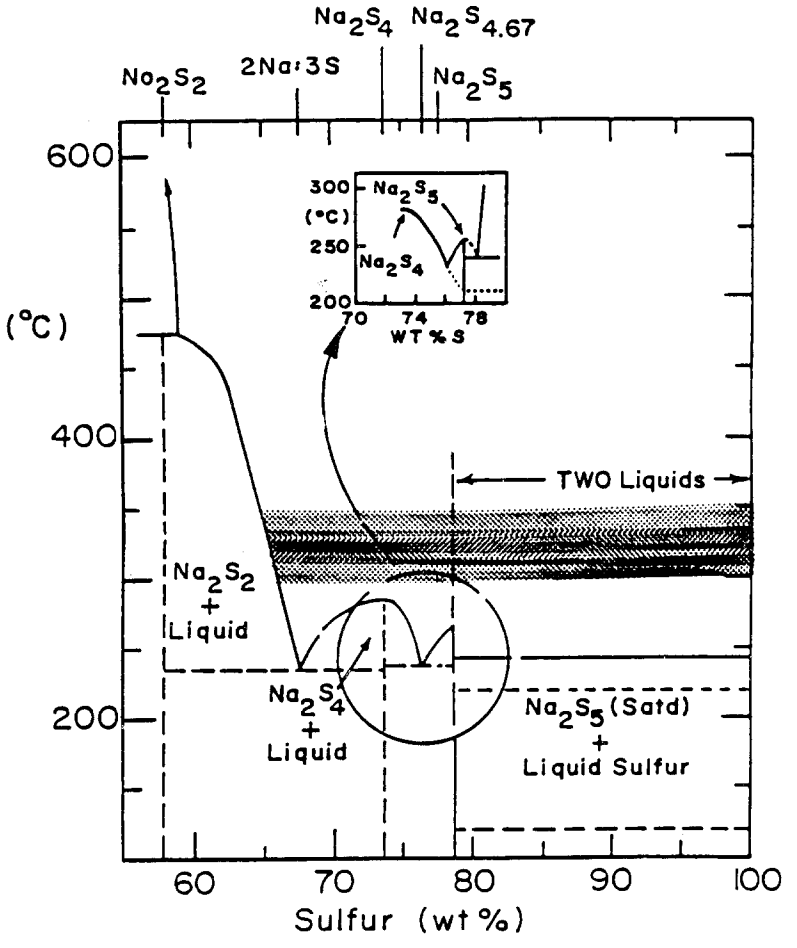

Fig. 1. The sodium–sulphur phase diagram for the composition range of interest when considering the sodium–sulphur battery concepts. Data from [1–3]. The shaded area for the temperature range 300–350° C, indicates the composition range for the system from complete charge (100% sulphur) to total discharge (~ 66% sulphur; i.e., the intersection of the liquid state field with the Na_2S_2 liquidus curve).

ible to follow thermal events as the material is thermally cycled, and this feature was an important consideration as an approach to the characterization of the melting–crystallization behaviour of the sulphur electrolyte. Further the DSC technique has been widely used with systems in which glass formation occurs, and this was an additional advantage relative to the present tasks. Our calorimetric facility centered around a Perkin-Elmer Model-2 DSC instrument, computer-aided through the Laboratory MicroSystems digital control system for automated data acquisition, base-line corrections, data analysis, and graphics for enthalpy and heat capacity measurements. The accuracy limits, established through energy calibration cross-checks with three metals (indium, tin, and lead) and two salt systems (KNO_3 and LiCl–KCl eutectic) were: temperature, ± 0.5° C, enthalpies, ± 1.0%; and heat capacities, ± 2.0%.

Melting temperatures were determined following the procedures noted below. Thus, for the isothermally melting materials (namely sulphur and the stoichiometric di, tri, tetra, and penta polysulphides) the T_m values were obtained by extrapolating the leading edge of the endotherm to the point of base-line intersection. The slope of the leading edge is a function of the thermal lag of the DSC calorimeter for isothermally melting materials. This is in contrast to non-isothermally melting systems, such as the non-stoichiometric (intermediate) compositions in the sulphur electrolyte system. For such systems the slowness of the melting process over-rides the thermal lag (above) so that the temperature range for the melting process may now be gained from the baseline intersections of the leading and trailing edges, respectively, and the apparent 'melting point' i.e., the point of maximum rate of melting is taken as the deepest point of the endotherm. The completion of the melting process is, nevertheless,

still defined as the point of return from the endotherm to the base-line. For mixtures, the measured enthalpies were normalized to the gram-mol concept using the overall compositions as the apparent 'molecular weights' of binary mixtures.

With the preceding guidelines, the enthalpies of solid-state transitions and melting, and the heat capacities of the materials as crystalline solids, and in the molten (liquid) states, were determined for sulphur and a series of polysulphide compositions spanning the composition range from Na_2S_2 to Na_2S_{10} (compositions higher than Na_2S_5 fall in the region of the two immiscible liquids composition area; refer: Fig. 1).

The measurements were made with heating and cooling rates set at 10° min^{-1}, and with a N_2 sweep rate through the assembly at $\sim 20\,cm^3\,min^{-1}$. The heat capacity data was acquired in overlapping 50° temperature increments spanning the total temperature range.

2.2. *Sulphur*

Elemental sulphur (reagent grade purity) was further refined in accordance with the requirements for the sodium–sulphur battery concept [4, 5].

2.3. *Sodium polysulphides*

Three techniques were used for the preparation of the sodium polysulphides, namely:

(a) reaction of sodium and sulphur under toluene [6–8];

(b) electrochemical reaction of sodium and sulphur [9, 10];

(c) 'in-capsule' DSC technique.

The third technique was developed in the present work and essentially reduces the macro-methods used by Rosen and Tegman [11] to microscopic methods so that the DSC capsule pans may be used directly as the reaction chambers for the preparation of the polysulphides, with Na_2S and sulphur as the reactants. In this approach the reactants were precisely weighed into the DSC pans in the exact amounts required for the desired product (polysulphide) by means of a high precision small mass measurement facility (such as a Cahn electro-balance). All transfers, weighings, and capsule crimp seals were performed in a dry and inert atmosphere.

The analytical methods for sulphide and polysulphide of Feher and Berthold [12] were used to confirm the molecular stoichiometries of the samples. The accuracy of the analyses was $\sim \pm 2\%$.

For the series of measurements of 'thermally aged' samples, an ancillary furnace at the operating temperature was used to maintain the encapsulated polysulphides at ~ 300–320° C for ~ 1500 h, and subsequently (in the same apparatus), at $\sim 200^\circ$ C for an additional period of ~ 1500 h.

In the work with the various additives, the in-capsule technique was also used. With water as the trace impurity, the dry atmosphere was exposed to moisture using a small amount of water in a (stoppered) flask. The additional weight gain of a pre-weighed amount of the polysulphide in the Cahn balance was then monitored, and the sample was crimp-sealed once the desired amount of moisture had thus been transferred to the sample. In a separate series, samples to evaluate the effect of carbon/graphite as additives were prepared in rigorously dry atmospheres using the polysulphide and carbon/graphite fibres, and the above direct-weighing micro-techniques.

3. Thermal data and fusion properties

3.1. *Sulphur*

The solid-state transition and melting point for sulphur of 'conventional' purity are generally reported as 95° and 115° C, respectively. In Fig. 2,

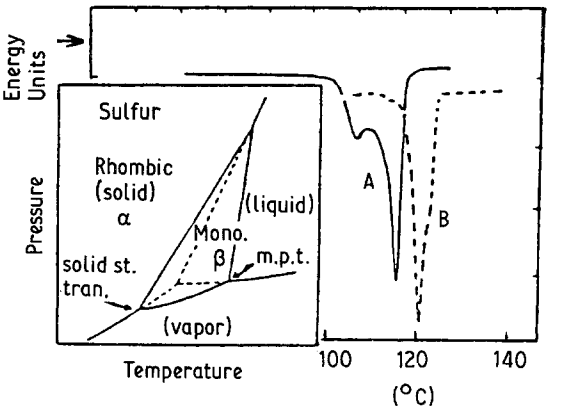

Fig. 2. Phase diagram and DSC endotherms for the sulphur melting process.

Table 1. Heat capacity of crystalline and molten sulphur

c_p; $C_p = a + bt + ct^2$ c_p(cal* g^{-1} deg^{-1}); C_p(cal* mol^{-1} deg^{-1})				
	a	$-b$ (X 10^3)	c (X 10^6)	S.E. (%)
rhombic sulphur (60–90° C)				
c_p	0.2822	4.040	33.87	~ 1.1
C_p	9.047	129.55	1085.99	~ 1.1
molten sulphur (120–165° C)				
c_p	1.432	19.56	79.49	~ 1.7
C_p	45.93	627.18	2548.86	~ 1.7
molten sulphur (165–337° C)				
c_p	0.7332	2.997	4.732	~ 1.5
C_p	25.31	96.10	151.73	~ 1.5

* For conversion to SI units, 1 cal = 4.184 J.

we show two DSC scans for the refined sulphur. Scan A illustrates the heating of rhombic sulphur. The first endotherm is for the solid-state transition of rhombic to monoclinic sulphur (~ 95° C), followed by the melting endotherm (~ 113° C). Scan B shows the heating of the same sample after the rhombic to monoclinic conversion was virtually completed in the solid-state. The solid-state transition endotherm is now absent, and the fusion process occurs virtually at the melting point of pure monoclinic sulphur. The melting point found, 118.1° C, corresponds closely with that reported by Feher *et al.* [13], i.e., 119.6° C. The heats of fusion are in exact agreement also, i.e., 3.06 kcal mol^{-1} (found); 3.07 kcal mol^{-1} [13].* The sulphur in the work of Feher *et al.* [13] was reported to be virtually all in the cyclooctastructural form. In the work of West [14] the sulphur was also of the highest purity (i.e., 99.999%), but the structural form(s) in the sample were not reported. The differences in heat of fusion value and the melting point observed by West [14] can be understood if the West sample was a mixture of two structures, the cycloocta- and catenaocta- forms of sulphur respectively. A portion of the enthalpy of reaction (conversion of catenaocta- to the cyloocta- form) would thus be included in the enthalpy of fusion observed by West; similarly the presence of the second structural form would depress the melting point. The heat capacity results for the highly refined sulphur are summarized in Table 1.

* For conversion to SI units, 1 cal = 4.184J

3.2. *Sodium polysulphides*

The fusion properties for a series of polysulphide compositions, from the disulphide to a composition that is well into the 2 immiscible liquids region (Fig. 1) are summarized in Table 2. The heat capacity data for the di-, tri-, tetra-, and penta-compositions, for the crystalline and molten states, and as supercooled liquids, are in Table 3a and b. The DSC scans illustrated in Fig. 3 show a series of sharp well-defined endotherms characteristic of the isothermal melting of crystalline ionic salts. These are for the '1st melting' of the polysulphides, freshly prepared from Na_2S and sulphur by the incapsule technique. This behaviour is not reproducible for polysulphide compositions above Na_2S_3. This is illustrated by the series of DSC scans shown in Fig. 4. Additional aspects of the melting–crystallization properties and behaviour may be summarized as follows.

3.2.1. Na_2S_2. Two solid state transitions are observed before the melting transition, i.e., at 50°–97° C, $\Delta H_{tr} = 190$ cal mol^{-1}; and at 117°–194° C, $\Delta H_{tr} = 240$ cal mol^{-1}. The melting point, 474° C, is that of an incongruently melting compound as seen by inspection of Fig. 1. The enthalpy of fusion (Table 2) is thus for the process:

$$Na_2S_2(c) \rightleftharpoons Na_2S(c) + Na_2S_{2.4}(\text{molten}).$$

The melting–crystallization behaviour does not change with repeated cycling; it remains the same

Table 2. Fusion properties for a series of sodium polysulphide compositions

Polysulphide composition	1st melting*		re-melting*		
	t_m (° C)	ΔH_{fus} (kcal mol^{-1})	*remelt cycles*	t_m (° C)	ΔH_{fus} (kcal mol^{-1})
Na_2S_2	474	1.78	3	474	1.73
$Na_2S_{3.0}$	234	3.72	3	234	3.72
$Na_2S_{3.3}$	–	–	2	241	5.67
$Na_2S_{4.0}$	283	6.87	3	240	5.98
$Na_2S_{4.2}$	–	–	3	207–234	4.12
			2	240–260	6.27
$Na_2S_{4.6}$	–	–	3	213–231	6.78
$Na_2S_{5.0}$	258	7.57	2	220–241	8.73
$Na_2S_{5.2}$ †	255	7.24	10	219–247	8.65
$Na_2S_{5.3}$ †	–	–	11	236–246	8.21
$Na_2S_{6.1}$ †	254	6.64	4	205–247	7.75
$Na_2S_{10.0}$ †	254	6.99	3	205–265	6.90

*The enthaply of 1st melting is that of the polycrystalline polysulphide prepared from the reactants, taken through the first fusion cycle; the enthalpy of re-melting is that for the same sample after repeated thermal cycling through the melting–crystallization temperature range.

†Compositions of higher sulphur content than $Na_2S_{5.0}$ enter a two phase region (see: phase diagram). For these compositions, on heating of crystalline solid, endothermic peaks attributed to sulphur melting were observed in the temperature range 100–120° C.

For conversion of ΔH to SI system of units, 1 kcal = 4.184 kilojoules.

as that observed in the '1st melting', i.e., the molten state cannot be supercooled to the glassy state; the maximum supercooling was ~ 40° below T_m (see Fig. 4a).

3.2.2. Na_2S_3. In the '1st melting', two solid-state transitions are observed, at virtually the same temperatures as for Na_2S_2 (3.1.1.) but with somewhat larger enthalpies, i.e., at 50°–98° C, ΔH_{tr} = 230 cal mol^{-1}; at 177–190° C, ΔH_{tr} = 1150 cal mol^{-1}. The value of the latter may be evidence of some chemical reaction occurring between Na_2S_2 and Na_2S_4 at this transition. As shown in Fig. 4b, the melting–crystallization properties may be reproducible for a few successive thermal cycles. This composition has the strongest tendency to supercool to the glassy state, and, once formed, the glass cannot be induced to crystallize. The glass transition temperature was observed to occur at 64° C.

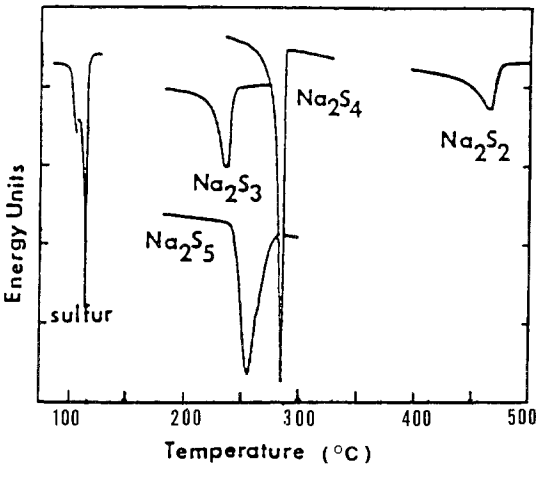

Fig. 3. DSC scans through fusion for sulphur and four sodium polysulphides.

3.2.3. Na_2S_4. After the '1st melting', the melting–crystallization behaviour changes to a melting point at ~ 240° C (cf: 283° C, 1st melting). Further, this composition shows the phenomenon of an inverse-crystallization exotherm; i.e., the melt supercools to a glassy state (the glass transition temperature is observed at ~ 73° C), and the crystallization exotherm is observed in the reheating cycle at ~ 132° C. Subsequently, melting is observed to occur at ~ 240° C. These features are illustrated in the DSC reheating scan shown in Fig. 5. This thermal pattern appears to be reproducible for more than 40 successive cycles through melting (see Fig. 4c). After a prolonged period at

Table 3a. Heat capacities for a series of sodium polysulphide compositions c_p; $C_p = a + bt + ct^2$, c_p (cal* g^{-1} deg^{-1}); C_p (cal* $mol\,g^{-1}$ deg^{-1})

	a	$-b$ ($\times 10^3$)	c ($\times 10^6$)	S.E. (%)
α-Na_2S_2; 97–167° C (*heat capacity is constant within experimental limits*)				
$c_p = 0.255$ (cal g^{-1} deg^{-1}); $C_p = 28.1$ (cal mol^{-1} deg^{-1})				
β Na_2S_2; 191–267° C (*heat capacity is constant within experimental limits*)				
$C_p = 0.265$ (cal g^{-1} deg^{-1}); $C_p = 29.2$ (cal mol^{-1} deg^{-1})				
β Na_2S_2; 267–437° C				
cp	2.497	14.80	24.61	~ 6%
Cp	274.89	1629.93	2709.9	~ 6%
Na_2S_3; 97–167° C				
c_p	0.1440	−0.495	–	~ 1.5%
C_p	20.47	−70.43	–	~ 1.5%
Na_2S_3; 187–207° C				
c_p	−0.8644	−6.204	–	~ 3%
C_p	−122.90	−882.0	–	~ 3%
Na_2S_4; 50–237° C (*heat capacity is constant within experimental limits*)				
$c_p = 0.219$ (cal g^{-1} deg^{-1}); $C_p = 38.1$ (cal mol^{-1} deg^{-1})				
Na_2S_5; 50–242° C (*heat capacity is constant within experimental limits*)				
$c_p = 0.207$ (cal g^{-1} day^{-1}); C_p (cal mol^{-1} deg^{-1}) = 42.8				

* For conversion of c_p, Cp to SI systems of units: 1 cal = 4.184 J.

300° C, the inverse-crystallization memory is lost, i.e., the glass state is retained throughout the thermal cycling.

One possible explanation of the fact that the melting point is 283° C on first fusion, and 240° C on subsequent fusion is that the glassy solid recrystallizes not to pure Na_2S_4, but to a mixture of crystalline solids (e.g., Na_2S_5, Na_2S_4 and

Table 3b. Heat capacities for a series of sodium polysulphide composition. Supercooled melts and in the molten state. Glass transition temperatures, T_g, *are:* Na_2S_3, 64° C; Na_2S_4, 73° C; Na_2S_5, 78° C; *with* Na_2S_4 *and* Na_2S_5 *crystallization onsets in the reheating step at 147° C and 109° C, respectively, i.e., these two-compositions show inverse-crystallization phenomena*

Polysulphide state	*temperature range* (° C)	c_p (cal g^{-1} deg^{-1})	C_p (cal mol^{-1} deg^{-1})
Na_2S_2 supercooled melt	Does not supercool to a glassy state		
molten state	467–500	0.333	36.7
Na_2S_3 supercooled melt	77–232	0.330	46.8
molten state	247–387	0.315	44.8
Na_2S_4 supercooled melt	82–147	0.333	58.1
molten state	287–387	0.317	55.3
Na_2S_5 supercooled melt	87–109	0.298	61.3
molten state	252–387	0.313	64.6

* For conversion of c_p, C_p to SI systems of units: 1 cal = 4.184 J.

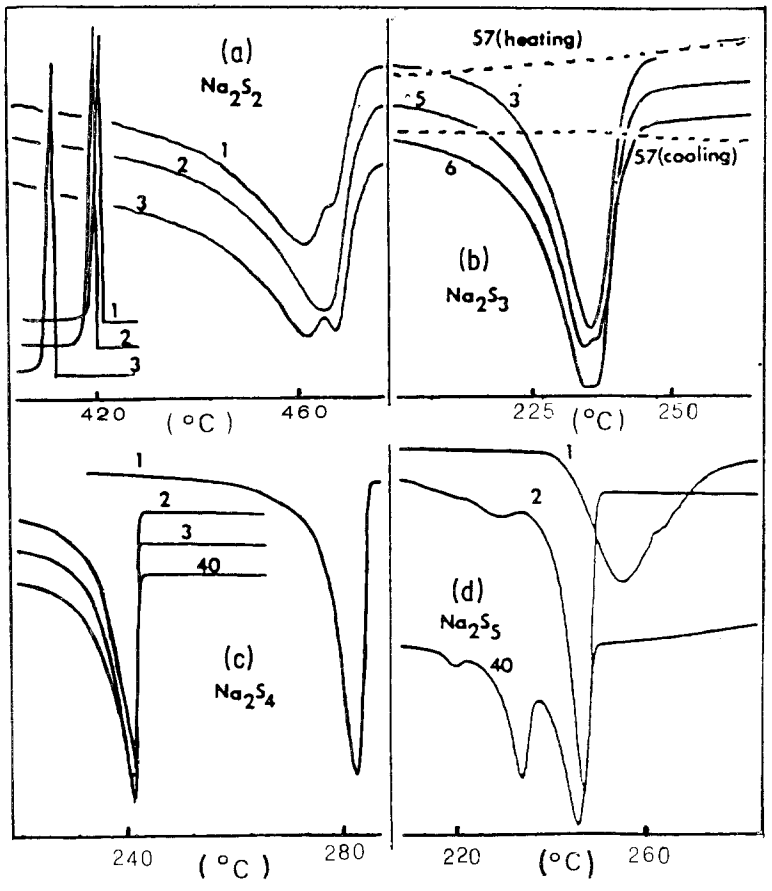

Figure 4. Effect of thermal-cycling on the melting characteristics of the sodium polysulfides. In Figure 4a, the upper curves are heating curves while the lower, are, correspondingly the cooling curves. Fig. 4b shows the heating curves for the 3rd, 5th, and 57th successive thermal cycles; in the 57th cycle, no thermal excursions (endothermic; exothermic) are observed in the heating and cooling cycles; in Figs. 4c and 4d, a series of heating cycles are shown to illustrate the changes in melting behaviour from those in the first melting cycle.

Na_2S_2). Inspection of the phase diagram (Fig. 1) shows that 240° C is close to the temperature of the eutectics in this system. This aspect was not pursued further in the present study.

3.2.4. Na_2S_5. The melting–crystallization properties change with the first melting in a similar manner to the observations for the tetrasulphide; the glass transition temperature is observed at 78° C; in the heating cycle, the crystallization exotherm occurs in the range: 116° C–160° C (i.e., inverse-crystallization phenomenon, cf., Na_2S_4). The melting process shows structure at ~ 219° C and 228° C; melting is complete at ~ 241° C. This behaviour appears quite reproducible; it has been observed after more than 40 successive thermal cycles; for DSC scans of the 1st, 2nd and 40th thermal cycles, see Fig. 4d. After an extended period in the molten state at ~ 300°–320° C, (~ 1500 h), this memory of crystallinity is still retained, as illustrated in the DSC reheating scan shown in Fig. 5. This behaviour is in contrast to the result for the tetrasulphide composition, where the memory of crystallinity was lost after a similar prolonged period at 300° C.

The series of endotherms in the DSC scans of remelt cycles of the pentasulphide composition may indicate premelting phenomena; alternately these may indicate the attainment of the three phase metastable system proposed by Rosen and Tegman [4] i.e., Na_2S_4(c), liquid eutectic, and (liquid) sulphur, mp. 227° C. A firm interpretation awaits further studies.

3.2.5. Non-stoichiometric compositions in the homogeneous liquid phase region. The melting–crystallization properties change with the first melting in a manner quite similar to that noted for pentasulphide compositions; i.e., a series of endotherms are observed in the fusion process, with the principle melting occurring approximately at that of the trisulphide eutectic composition.

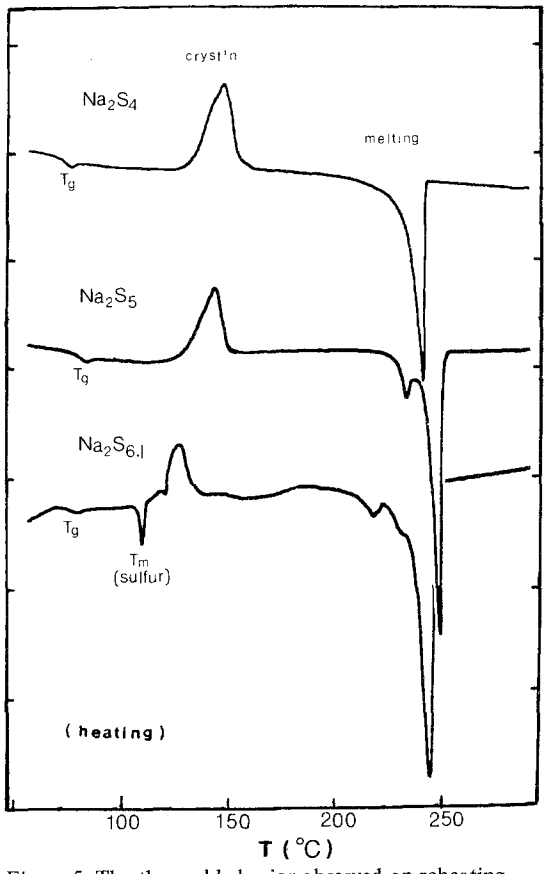

Figure 5. The thermal behavior observed on reheating, from room temperature, for Na_2S_4 and Na_2S_5 and for one composition in the region of liquid-liquid immiscibility, i.e., $Na_2S_{6.1}$. All samples were "aged" by repeated thermal-cycling. Na_2S_4 retained its memory of crystallinity for ~ 170 hrs at 300° C; Na_2S_5 still followed this behavioral pattern after ~ 1500 hrs. at 300°–320° C; in the two immiscible liquids region (e.g., $Na_2S_{6.1}$) the behavioral pattern appears to be a composite of those of elemental sulfur and pentasulfide.

3.3. *Melting–crystallization properties after 1500 h at 300°–320° C*

The behaviour of sulphur was essentially the same as prior to this prolonged period at ~ 300° C. Na_2S_3 showed no memory of crystallinity; the glass transition was observed at 64° C. Na_2S_4 had lost its memory of crystallinity in the first 170 h at 300° C. The pentasulphide, by comparison, exhibited the same melting–crystallization behaviour as reported above, i.e., the 'memory' of crystallinity again appeared in the heating cycle as an inverse-crystallization phenomenon at ~ 121° C, and fusion then followed from 220–241° C, (see: Fig. 5, Na_2S_5 reheating DSC scan).

3.4. *Two immiscible liquids region*

The melting–crystallization behaviour in this range could be clearly characterized as that of sulphur superimposed on that of Na_2S_5; the DSC reheating scan for the overall composition, $Na_2S_{6.1}$ shown in Fig. 5, illustrates this. Heat capacity measurements were undertaken for one composition in this region, namely $Na_2S_{6.1}$. Within the experimental limits of error, the heat capacities corresponded with the values predicted from mole-fraction additivity (with Na_2S_5 and sulphur as parents). The melting temperature (ranges) and the corresponding enthalpy changes have already been noted elsewhere in this work (Table 1).

The saturation solubilities for sulphur in the molten Na_2S_5 layer were derived from the fusion data and an iterative calculation based on the van't Hoff freezing point depression principle. These results are in Table 4. The saturation solubility for sulphur in the molten polysulphide is thus ~ 0.32 wt%. A similar analysis of the data for the sulphur layer was attempted but, owing to an overlap of the solid-state transition with the melting process, quantitative results could not be obtained.

3.5. *Effects of additives as trace impurities*

The effects of two additives, carbon/graphite fibres, and moisture, on the melting–crystallization behaviour of the polysulphides were investigated separately using the 'in-capsule' DSC technique and the $Na_2S_{3.3}$ composition as 'host'. For the addition of carbon/graphite fibres (0.0 to ~ 8.0

Table 4. Saturation solubilities of sulphur in Na_2S_5 in the two immiscible liquid composition ranges

Sample stoichiometry	*Sulphur solubility* (mg S/g Na_2S_5)
$Na_2S_{5.0}$	0.06*
$Na_2S_{5.2}$	3.4
$Na_2S_{6.1}$	3.2
$Na_2S_{10.0}$	3.0

* The composition Na_2S_5 lies outside the two-immiscible liquids composition range. The solubility of sulphur would be vanishingly small, i.e., zero. The above value (0.06) thus indicates the limits of accuracy of the analytical technique.

wt%), virtually no changes could be detected, using the melting temperatures and the enthalpies of fusion sensors. Further, nucleation of the supercooled liquid was not induced by the presence of these fibres as additives; i.e., the melts supercooled to the glass state, (cf. $Na_2S_{3.3}$, Table 2).

The results with water as the additive are summarized in Table 5. Absorption of moisture leads to the formation of Na_2O, NaOH, and H_2S as reaction products. Inspection of the results (Table 5) shows that moisture, even in quite small amounts, has a marked effect on both the melting temperatures (ranges) and the accompanying enthalpies of fusion. With these parameters as sensors, the DSC method appears of promise as an analytical technique for determinining sample purities.

3.6. *Chemical processes*

The thermicity for the following series of processes were monitored by the DSC technique, using direct weighing of the reactants into the calorimetric capsules, i.e., the 'in-capsule' DSC technique.

disulphide: $Na_2S + S \longrightarrow Na_2S_2$ (1)

trisulphide: $Na_2S + 2S \longrightarrow Na_2S_3$ (2)

tetrasulphide: $Na_2S + 3S \longrightarrow Na_2S_4$ (3)

pentasulphide: $Na_2S + 4S \longrightarrow Na_2S_5$ (4)

The DSC scans illustrated in Fig. 6, show that the endothermic and exothermic effects can be grouped collectively in three general zones: a sulphur melting zone; a chemical reaction zone; and a polysulphide melting zone. The temperatures and enthalpy effects accompanying these events are summarized in Table 6. It should be noted the temperature ranges for exothermic events correspond closely to the solid-state 'tempering steps' empirically advanced by Rosen and Tegman for the preparative synthesis of these materials [4, 15].

4. Discussion

The calorimetric measurements revealed a number of unexpected and unusual features. Some of these briefly, are as follows.

The disulphide, on heating, undergoes a reaction to form Na_2S (solid phase) and a molten polysulphide (liquid phase). The fusion process is thus merged with the phase reaction for Na_2S_2 as an incongruently melting compound.

The melting temperatures of polycrystalline Na_2S_4 and Na_2S_5 are reproducible only for the 1st melting cycle. Subsequently, these materials exhibit melting–crystallization properties closely similar to those of the eutectic compositions (e.g., Na_2S_3).

With the exceptions of the disulphide, all polysulphides 'lose memory' of crystallinity on repeated thermal cycling, *or* after prolonged periods in the molten state, i.e., in the cooling step, these materials exhibit no exothermic events and pass smoothly from the liquid state, through the supercooled liquid state, and into a glass state. Glass-transition temperatures are exhibited and have been characterized. Inverse-crystallization temperatures are observed for some of these glasses. The latter corresponds to a spontaneous onset of crystallization as the glassy state is warmed to progressively higher temperatures from room temperature.

The fact that supercooling and glass formation readily occur in the middle part of the compo-

Table 5. Effect of moisture on the melting behaviour of sodium polysulphide samples

Polysulphide composition	ΔH_2O (wt %)	t_m (° C)	*Melting range* (° C)	ΔH_{fus} (kcal mol^{-1})
$Na_2S_{3.3}$	0.00	241	233–353	5.74
$Na_2S_{3.3}$	0.34	240	226–255	5.16
$Na_2S_{3.3}$	1.05	234	212–260	4.44
*$Na_2S_{2.5}$	2.20	234	202–263	3.81

* Sample absorbed moisture either during preparation or storage. For conversion of ΔH to SI system of units, see Table 2.

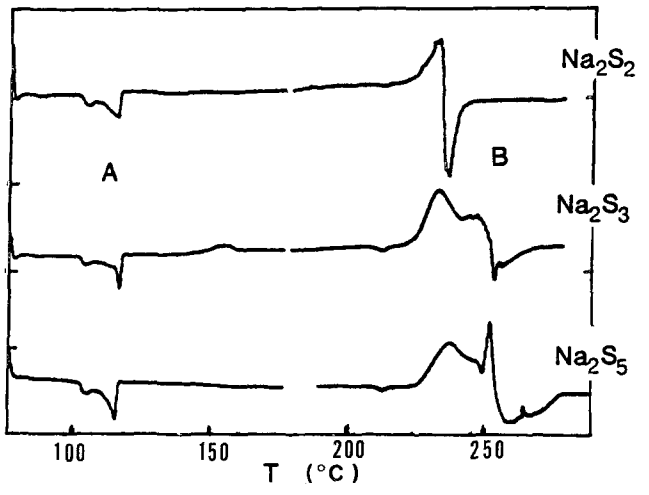

Figure 6. DSC scans illustrating the thermicity of the reaction of Na_2S sulfur to form the di-, tri-, and penta-sulfide compositions. A; sulphur melting zone; B: chemical reactions zone.

sition range raises some questions whether due cognizance of this as a possible error source was shown in the original phase diagram studies [1–3]. On this point, inspection of the studies of Rosen and Tegman [3] shows that the observations were based on visual methods (hot-stage microscopy and DTA), and supported by X-ray powder diffraction data. Further, the samples were 'tempered' as already noted to gain polycrystalline materials (the 'tempering' was, in each case, at a temperature found to be above the inverse crystallization temperatures observed in the present work). These investigators also noted the above tendencies to super-cooling and glass formation and, indeed,

Table 6. Thermally initiated processes in the reaction of Na_2S and elemental sulphur. A, sulphur melting zone; B, chemical reactions zone; C, polysulphide melting zone.

	Zone					
	← A →		← B →		← C →	
t (° C)	102	112	222	234	466	468
ΔH						
(kcal mol^{-1})	2.86		0.58	0.75	0.003	0.043
Thermicity	endo-		exo-	endo-	endo-	endo-
$Na_2S + 2S = Na_2S_3$	← A →		← B →		← C →	
t (° C)	101	111	154	212	224 240	252
ΔH						
(kcal mol^{-1})	2.82		0.31	0.052	3.13	0.82
Thermicity	endo-		exo-	endo-	exo-	endo-
$Na_2S + 3S = Na_2S_4$	← A →		← B →		← C →	
t (° C)	102	114	220	247		279
ΔH						
(kcal mol^{-1})	2.37		6.50			4.49
Thermicity	endo-		exo-			endo-
$Na_2S + 4S = Na_2S_5$	← A →		← B →		C →	
t (° C)	102	113	213	226	248	253
ΔH						
(kcal mol^{-1})	3.40		0.09	5.54		4.41
Thermicity	endo-		endo-	exo-		endo-

For conversion of ΔH to SI system of units; see; Table 2.

found that most of the useful information was to be gained from fusion observations, rather than freezing measurements. In the work of Gupta and Tischer [1], an equilibrium emf technique (formation cells) was used. It appears that there is firm support for the reliability of the phase diagram (Fig. 1) for this system.

Cohen and Turnbull [16, 17] proposed that the glass transition temperature, T_g should be roughly proportional to cohesive energy. Thus, when two substances of approximately equal cohesive energies mix to form a eutectic system, the T_g should be roughly independent of composition. Also the amount of supercooling (to attain the glass state) should be least at the eutectic composition. Inspection of the thermal cycling behaviour for the sodium polysulphides shows that the supercooling characteristics and glass forming tendencies correlate closely with the preceding generalizations. One also notes that the ratio, T_g/T_m, for Na_2S_2 is ~ 0.44, whereas for the higher polysulphides, this ratio falls in the range of ~ 0.66. According to Turnbull [18], if the value of (T_g/T_m) for a material falls much below 0.66, the material will not have glass forming tendencies. The melting–crystallization behaviour for Na_2S_2 observed in the present study is in accord with this.

Ubbelohde has attributed the propensity for glass formation as due to an onset of 'anticrystallinity' in the molten state of that material, [19, 20], i.e., a structural aggregation of the species in the form of non-crystallizable clusters onsets in the liquid state. This aggregation is in competition with the domains (or micro-regions) that normally act as nucleation sites for crystallization. If anti-crystallinity becomes dominant, the material supercools to the glassy state. The melting–crystallization behaviour of the polysulphides is thus in part understood as being due to some unique structural features in this class of materials. The sodium cations can be thought of as being 'separated' or 'shielded' by larger polyatomic polysulphide anions, i.e., by 'slices' of non-branching, non-planar chains of sulphur atoms, much as in 'ionic-sandwich' structures. Such arrangements appear to promote anti-crystalline clustering of the species in the molten state, and this appears to be dominant in the polysulphide compositions for which the glassy state is realized on cooling from the molten state.

Acknowledgements

This work was made possible, in a large part, by the support received from the U.S. Department of Energy, Washington, D.C.

We acknowledge with pleasure the assistance of Giai Truong with the calorimetric measurements and particularly in the heat capacity measurements.

References

[1] N. K. Gupta and R. P. Tischer, *J. Electrochem. Soc.* **119** (1972) 1033.
[2] D. J. Oei, *Inorg. Chem.* **12** (1973) 435.
[3] E. Rosen and R. Tegman, *Chemica Scripta* **2** (1972) 221.
[4] 'Review of U.S. Department of Energy/Ford Sodium Sulfur Battery Program', April (1980); Ford Aerospace and Communications Corp. Newport Beach, California.
[5] 'Review of Advanced Battery Development Program for Electric Utility Applications', April, (1980); General Electric Co., Energy Systems Programs Dept., Schenectady, New York.
[6] J. Locke and A. Austell, *Amer. J. Sci.* **20** (1898) 592.
[7] T. G. Pearson and P. L. Robinson, *J. Chem. Soc.* **19** (1931) 83.
[8] F. Feher and H. J. Berthold, *Zeit. Anorg. Allg. Chemie* **273** (1953) 144.
[9] K. D. South, J. L. Sudworth and G. Gibson, *J. Electrochem. Soc.* **119** (1972) 554.
[10] B. Cleaver and M. D. Davies, *Electrochim. Acta* **18** (1973) 733.
[11] E. Rosen and R. Tegman, *Acta Chem. Scand.* **35** (1971) 3329.
[12] F. Feher and H. J. Berthold, *Fresenius Zeit. Anal. Chemie* **138** (1953) 245.
[13] F. Feher, G. P. Gorler and H. D. Lutz, *Zeit. Anorg. Allg. Chemie* **382** (1971) 135.
[14] E. D. West, *J. Amer. Chem. Soc.* **89** (1959) 29.
[15] R. Tegman, Ph.D. Thesis, Univ. Umea, Sweden (1974).
[16] M. H. Cohen and D. Turnbull, *J. Phys. Chem.* **34** (1960) 120.
[17] *Idem, Nature* **189** (1961) 131.
[18] D. Turnbull, *Contemporary Physics* **10** (1969) 473.
[19] A. R. Ubbelohde, 'Melting and Crystal Structure', Clarendon Press, Oxford (1965).
[20] *Idem,* 'The Molten State of Matter', Wiley-Interscience Inc., New York (1976).